POLITECNICO
MILANO 1863

SCUOLA DI INGEGNERIA INDUSTRIALE
E DELL'INFORMAZIONE

Executive Summary of the Thesis

Design and implementation of a laser measurement system for loudspeaker vibrational behaviour characterization

Laurea Magistrale in Music and Acoustic Engineering - Ingegneria Acustica e Musicale

Author: Lorenzo Lellini

Advisor: Prof. Giuseppe Bertuccio

Co-advisor: Dott. Marco Zanettini

Academic year: 2022-2023

1. Introduction

Designing a loudspeaker requires to carefully consider various factors for optimal performance and to analyze vibrating membranes helps designers make informed choices. A reliable instrument using a Laser Doppler Vibrometer captures detailed vibration data, providing valuable insights into loudspeaker performance. This work aims at creating an easy-to-use measuring tool providing useful information on loudspeakers membranes vibrational behaviour in order to verify the correct design or to highlight design errors or defects in the used materials. The instrument is developed from [1], and, although similar instrumentation already exists on the market, this work is focused on creating a similar tool with a higher level of customization and much lower costs. To measure membrane displacement without perturbing its behaviour, a non-contact measurement technique using a laser displacement sensor based on triangulation principles was preferred over more traditional approaches using accelerometers or similar sensors. In order to properly characterize the vibrational behaviour of the whole radiating surface over an extended frequency range, the choice of both stimulus signal and measurement points grid is critical. Calculating acceleration from the measured displacement signal, sound pressure level (SPL) and accumulated acceleration level (AAL) can be predicted with good approximation using Rayleigh's integral.

2. Causes of a nonlinear behaviour in loudspeakers

Electrodynamic or moving-coil loudspeakers are devices converting electrical signals into sound. They are made up of various components such as a diaphragm or cone, a dust cap, a coil, a magnetic gap with a pole piece and pole plate, a permanent magnet, a basket structure and suspensions (a surround in the upper part of the cone, and a spider in the lower part of the loudspeaker). When an audio signal is applied to the electrical connections, the current interacts with the magnetic field, causing the voice coil and cone to move, oscillating air molecules and producing sound waves. Loudspeaker can be modeled as an interaction between electrical, mechanical, and acoustical domains, resembling a mass-spring-damper system from a mechanical perspective. By using analogies between these domains, a circuit representation of the loudspeaker can be created, considering all three as-

pects [2]. The focus of this work is to characterize the loudspeaker from a vibrational perspective rather than analyzing it from a circuit point of view. While the electrical aspect is important, the emphasis will be on understanding the vibrational behaviour, frequency response, and other essential parameters that are interconnected and collectively contribute to the overall response of the loudspeaker. The choice of materials and shapes of the components greatly affects performance: low-frequency professional loudspeakers typically use a diaphragm made of treated paper, while high-frequency ones use materials such as titanium, aluminum, or beryllium. At high frequencies, vibrations and resonances in the cone can introduce irregularities in the frequency response curve and influence sound radiation patterns. Loudspeaker designers would greatly benefit from a measurement instrument allowing them to analyze membranes complicated vibrational behaviour, to properly assess and quantify the importance of both geometry and materials on radiated sound.

2.1. Membrane vibrational behaviour

Circular plates exhibit various wave patterns called modes. The circular shape of the plate and the fixed boundary conditions at the outer edge significantly impact the behaviour of waves within the plate. This radial symmetry allows waves to propagate in all directions, resulting in nodal patterns with rotational symmetry [2]. Moving on to loudspeakers, their mechanical properties, including the cone material, suspension material, mass per area, stiffness, damping, and speaker geometry, greatly influence their frequency response. These properties affect the mechanical vibrations experienced by the loudspeaker. At lower frequencies, the cone tends to move as a whole, due to its stiffness. As the frequency increases, the cone undergoes mechanical bending and longitudinal waves, by bringing it to the break-up frequency and the emergence of a complex vibration pattern. To better understand the vibrational behaviour of the loudspeaker membrane, different measurement grids have been tested. Studying these patterns, designers aim to accurately characterize the membrane's response. By decomposing the total loudspeaker displacement in in-phase, anti-phase and quadrature, it becomes possible to analyze the contributions of the individual vibration modes and understand their combined effect on the overall response [3].

2.2. Loudspeaker cone modal decomposition

Evaluating vibrational modes relative contribution to radiated sound is very important to design loudspeakers with the desired response and several decomposition techniques can be used for this aim. For instance, phase decomposition can be conveniently used to separate complete vibration into in-phase, anti-phase and quadrature components according to their contribution to total radiated sound. Additionally, decomposing cone vibrations into radial and circular components can help identify "acoustically harmful" modes potentially decreasing device performance. The measured loudspeaker displacement $x(r, \theta)$, expressed in polar coordinates and depending on radius r and angle θ, can be thus expressed as decomposition of radial and circumferential modal components [3]:

$$x(r, \theta) = x_{circ}(r, \theta) + x_{rad}(r) \tag{1}$$

Radial component generates the dominant contribution to the on-axis SPL while circular component has a negligible effect on the total SPL radiated on-axis [4]. The focus of this work is not to decompose the displacement of a loudspeaker into radial and circular modes but to analyse the decomposition of the cone displacement of a loudspeaker into in-phase, anti-phase and quadrature components.

3. Input signal generation and IR computation

An the exponential sine sweep excitation signal has been used to excite the membrane in a certain range of frequencies between f_1 and f_2 [5]. Since vibration amplitude decreases with frequency, a growing 6 dB/oct amplitude shaping was applied to the sine sweep. With this choice, the inverse convolution filter $g(t)$ ends up having constant amplitude with time. Since loudspeaker is a nonlinear system, a synchronization procedure is needed to separate distortions from the fundamental [5]. The voltage to displacement *Transfer Function Impulse Response* can be easily calculated by performing

a convolution with the inverse sine sweep filter $g(t)$ derived from $x(t)$. The obtained $h(t)$ is later transformed in the frequency domain and used to compute the voltage to acceleration *Transfer Function*. Since latency in the sound card used to acquire the laser displacement sensor signal is not constant, impulse responses were aligned in post processing phase by using the `finddelay` MATLAB function.

4. Measurement grid

Different measurement grid layouts can be chosen depending on the desired spatial resolution over the radiating surface. Two types of grid have been designed: a denser one to have a *detailed scan* and a wider one to have an *exploratory scan*. The exploratory scan divides the cone in 30 radii (12 degrees between each radius) of 15 measurement points each for a total of 450 measurement points. The detailed scan divides the cone in 80 radii (4.5 degrees between each radius) of 40 measurement points each for a total of 3200 measurement points. Moreover, points density can be varied along the radial coordinate to better characterize the outer suspension (surround) behaviour.

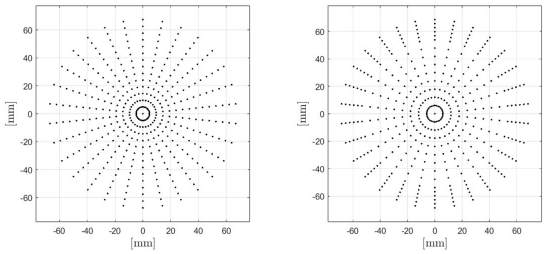

Figure 1: Exploratory grids: regular spacing on the left and non regular spacing on the right.

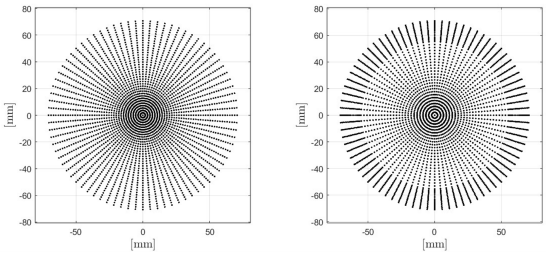

Figure 2: Detailed grids: regular spacing on the left and non regular spacing on the right.

5. Sound Pressure Level (SPL) and Accumulated Acceleration Level (AAL)

Approximating the loudspeaker as a flat piston in a rigid infinite baffle, the Kirchhoff-Helmholtz integral reduces to the Rayleigh integral:

$$p(\omega, r) = \frac{\rho_0}{2\pi} \int_{S_c} \frac{A(\omega, r)}{|r_a - r_c|} \, e^{-jk|r_a - r_c|} \, dS_c \quad (2)$$

where ρ_0 is the standard air density, $k = 2\pi f/c$ is the wavenumber, where c is the standard sound speed in air, S_c is the total diaphragm surface, r_a is the coordinate of the point where the sound pressure is calculated with respect to the loudspeaker diaphragm axis, r_c is the distance between the coordinate of the point where the measurement is performed with respect to the diaphragm center (it depends on the measurement grid) and $e^{-jk|r_a - r_c|}$ is the Green function taking in account the phase delay due to the distance between the measured point and the listening point where the SPL is computed. Sound Pressure Level is then defined as:

$$SPL(\omega, r) = 20 \log_{10} \left(\frac{|p(\omega, r)|}{\sqrt{2} p_0} \right) \, [dB] \quad (3)$$

where p_0 is the standard air pressure. In order to quantify the ideal maximum sound pressure level which could be produced if all points on the radiating surface moved in-phase, two additional quantities disregarding phase differences can be defined, respectively called accumulated acceleration and Accumulated Acceleration Level (AAL):

$$a(\omega, r) = \frac{\rho_0}{2\pi} \int_{S_c} \frac{|A(\omega, r)|}{|r_a - r_c|} \, dS_c \quad (4)$$

$$AAL(\omega, r) = 20 \log_{10} \left(\frac{a(\omega, r)}{\sqrt{2} p_0} \right) \, [dB] \quad (5)$$

Both quantities are related to the loudspeaker mechanical energy, whether this gets translated into sound or not. Comparing AAL and SPL, problematic behaviour in particular frequency ranges can be spotted, design flaws can be identified and corrected to improve the device performance. The distance $|r_a - r_c|$ is computed

taking into account the position of the i-th point at distance r_c on the radius and the distance r_a to the reference point where the SPL and the AAL are computed, as shown in figure 3.

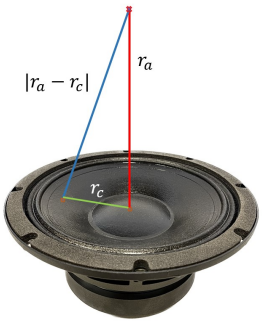

Figure 3: Distance between the i-th measured point on the radius at a distance r_c from the cone center and reference point r_a where AAL and SPL are computed.

In figure 4 a comparison between AAL and SPL on a 6 inches woofer is shown. We can immediately see how the two curves start to be increasingly different above the break-up frequency. Below the break-up frequency, the loudspeaker is in the **piston mode regime**: the cone is sufficiently stiff to move as a whole and all the cone parts move in-phase. Above the break-up frequency different vibration modes appear and some parts of the cone start moving out of phase with respect to the others.

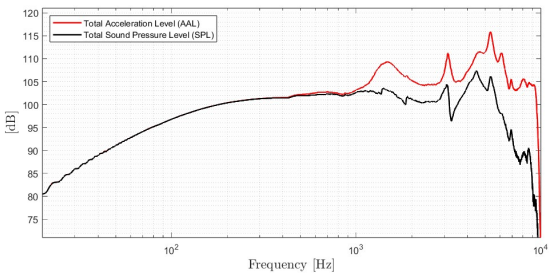

Figure 4: Total Accumulated Acceleration Level and total Sound Pressure Level comparison. In this case, the break-up frequency is around 1000 Hz.

In order to compute the Rayleigh integrals 2 and 4, we need to consider the whole measured surface S_c. For this calculation, the behaviour of every point was assumed to be representative of the surrounding area. In particular, the surface was divided in as many circular rings as points on each radius, and in as many slices as radii in the measurement grid.

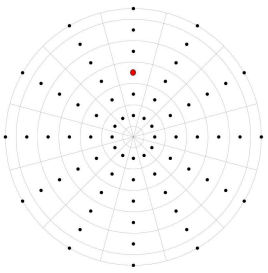

Figure 5: Cone area subdivision.

5.1. In-phase, anti-phase and quadrature components

Any vibration can be expressed as the sum of three components according to the phase relation with the total sound pressure as calculated in the reference point [6]. The in-phase component constructively contributes to the total radiated sound pressure, the anti-phase component destructively contributes to sound radiation and the quadrature component does not contribute to sound radiation at all. The total complex cone vibration displacement of each point on the cone surface can thus be expressed as:

$$x_{total} = x_{in} + x_{anti} + x_{quad} \tag{6}$$

The reference phase of the in-phase displacement component for each point on the surface can be calculated as:

$$\varphi_{ref} = \varphi_p + k|r_a - r_c| + \pi \tag{7}$$

where φ_p is the phase of the pressure (eq. 2), k is the wavenumber and an additional phase shift of π has been added from the phase difference between the displacement and the acceleration of the surface. Considering the *Transfer Function* $X(\omega, r)$, it is possible to calculate the in-phase, anti-phase and quadrature contribution of each measurement point:

the **in-phase** contribution is defined as:

$$x_{in} = \mathfrak{Re}_+ \left[X(\omega, r) \cdot e^{-j\varphi_{ref}} \right] e^{j\varphi_{ref}} \tag{8}$$

the **anti-phase** component is defined as:

$$x_{anti} = \mathfrak{Re}_- \left[X(\omega, r) \cdot e^{-j\varphi_{ref}} \right] e^{j\varphi_{ref}} \tag{9}$$

the **quadrature** component is defined as:

$$x_{quad} = \mathfrak{Im}\left[X(\omega, r) \cdot e^{-j\varphi_{ref}}\right] e^{j(\varphi_{ref}+\frac{\pi}{2})} \quad (10)$$

In figure 6 we can see the three components decomposition for a given measurement point.

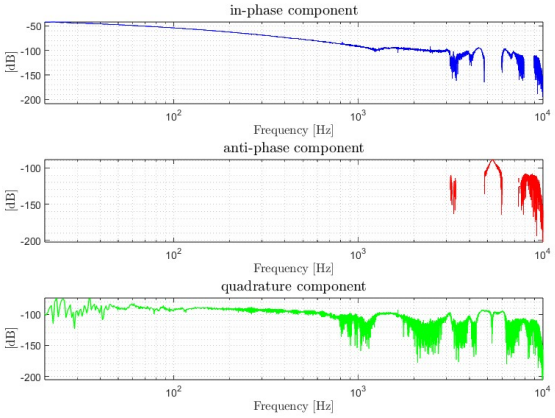

Figure 6: In-phase, anti-phase and quadrature components in frequency.

Once components have been computed for all the cone surface, their AAL and SPL can be calculated using formulas presented in section 5. As it can be appreciated, the in-phase and anti-phase AALs are equal to the in-phase and anti-phase SPLs. Please note that, while single points "in quadrature" contributions to the total SPL are not null, their sum (integrating all over the surface) is null.

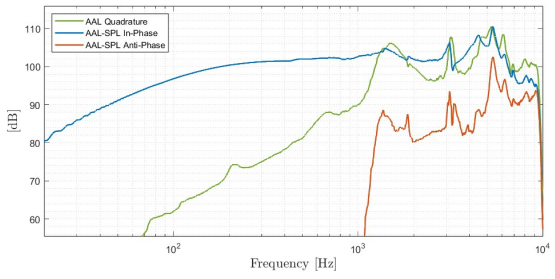

Figure 7: Components AAL and SPL.

5.2. Components graphical visualization

In order to visually analyze the vibration behaviour, the in-phase, anti.phase and quadrature components can be superimposed over the surface profile. As shown in figure 8, at low frequencies the diaphragm is in **piston mode regime** and moves as a whole due to its stiffness.

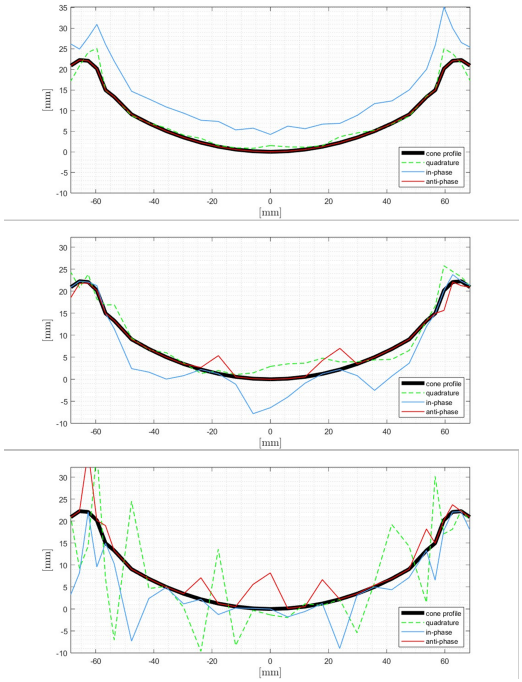

Figure 8: Components real part plot along a cone diameter. From top to bottom: 300 Hz, 1500 Hz and 5000 Hz.

6. Experimental setup design and implementation

The instrument design is inspired on [1] but, instead of designing a dedicated mechanical structure including dedicated motors and mechanical constraints, an **EPSON Scara T3** industrial robot coded in **EPSON SPEL+** language has been used. The operating principle is moving a laser on a cone surface according to the points of a grid, defined in section 4, and, by properly varying the distance between the laser displacement sensor and the surface so that their relative distance always falls into the measurable range, using the sensor output signal to retrieve the displacement of each grid point. The stimulus signal (section 3) is amplified with a **Powersoft K20** amplifier before being sent to the loudspeaker. The acquisition is carried out by connecting the laser sensor output to a **MOTU M4** sound card and reading the output voltage value from it. Both acquisitions and signals post processing are performed in **MATLAB**. All the laser measurements are stored as 64 bit floating point files.

Finally, the computed total SPL[1] using formulas 2 and 3 is compared with SPL measurement performed in anechoic room (figure 9) where the loudspeaker is placed in a large closed box that is an approximation of the infinite rigid baffle. Not being the box infinitely extended, some deviation between the measured and calculated SPL is expected, specially at the low frequencies.

Figure 9: SPL measurement in anechoic room with a free-field pressure microphone.

In order to measure and correctly set the amplifier output voltage, a **Fluke 289** multimeter has been connected to the amplifier output before starting the measurement. During the measurement, the loudspeaker is fixed on an horizontal surface with a **mandrel** in order to avoid undesired structural vibrations and to have a fixed central reference point for the measurement grid. In order to attach the laser sensor to the robot arm, a **3D printed bracket** was realized starting from a customized **Solidworks** CAD drawing. The cone surface is treated with a white **3D scanning powder** in order to improve light reflection and consequently the laser signal to noise ratio. Several tests have been performed and a better SNR is obtained whenever a white painted surface is used. Other treatment materials have been tested, but the added mass or the grains of dust crumbling and flying through the laser beam make the measurement unreliable.

[1]SPL and AAL in formulas 3 and 5 are calculated considering the reference point at ad distance of 1 m on loudspeaker axis.

Figure 10: Loudspeaker cone treated with white 3D scanning powder.

The used laser head model is **Keyence LK-G32** with a 655 nm emission. The laser sensor controller, needed for proper signal conditioning, is connected to an external 24 V power supply. The sensor focal range is ± 5 mm, the output is set to ± 10 V (gain is thus set to $2V/mm$) and it is connected to the sound card input via XLR cable. The laser sampling frequency is set to 50 kHz and no moving average filter is used. Keyence **LK-Navigator** software is used to set the laser controller parameters and check the sensor distance from the loudspeaker cone surface. During the measurement, the robot needs to move the laser sensor along the Z axis according to the loudspeaker cone profile to keep their distance inside the accepted range. Since the robot software, the laser software and MATLAB does not communicate each other, programming the robot to behave as explained was a very challenging part of this work. A solution was found calculating the Z axis coordinate of the robot starting from the loudspeaker CAD drawing. In fact, due to the AC-coupling characteristics of the sound card inputs, no direct measurement of the cone profile using the displacement sensor is possible.

7. Analysis of results

In order to test the measurement instrument, two 6 inches loudspeakers have been used as test samples. Both the loudspeakers share the same identical components and design except the spider suspension, which in one case is stiffer. All measurements lasted 5 seconds, several grids layouts have been tested and frequencies in the 10 Hz - 10000 Hz have been analyzed. For the stiffer loudspeaker all the grids in figures 1 and 2 have been tested. For the more compliant loud-

speaker, two measurement were performed: an exploratory grid with higher points density on the edge (figure 1 on the right) and one with another grid pattern with 792 measurement points on 22 radii (36 points for each radius with 2 mm constant spacing). It has been also verified how AAL and SPL change in function of the number of radii we are taking into account.

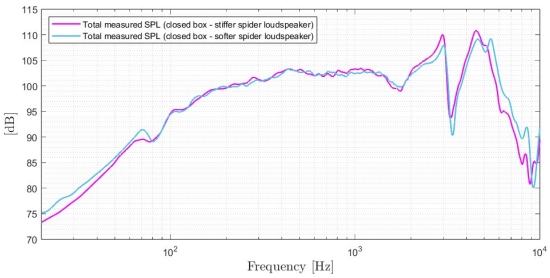

Figure 11: Closed box measured SPLs for loudspeakers equipped with stiffer and softer spider. Small differences are observed after 2000 Hz.

The first interesting result is that AALs of the flat cone surface approximation and CAD geometry surface coincide for each different measurement grid. This was an expected result because, since AAL does not takes into account the phase, the distance between the measured points and the observation point $|r_a - r_c|$ does not affect the phase[2]. Moreover, measurements performed with detailed grids show better agreement with the anechoic room measured SPL than measurements performed with exploratory grids do. Measurements results of the loudspeaker with the softer spider have been compared with the ones of the commercial instrument machine [1]. To compare the results obtained with the commercial hardware as closely as possible with those obtained with the in-house developed instrument, a 451 measurement points grid was used to perform the scan with the commercial hardware and a 450 measurement points grid with non constant points spacing on the radius (higher points density on the edge). AALs curves are almost identical. The small differences between them can be caused by several factors such as:

- Different loudspeaker measuring position that could not be properly centered in the same way.
- Since both compared grids have 30 radii at 12 degrees each, the two measurements could be performed on a different rotation angle and thus considering different radii with a slightly different modal behaviour.

[2]The small variations of the distance $|r_a - r_c|$ due to the differences between the CAD geometry and the real profile of the cone are negligible.

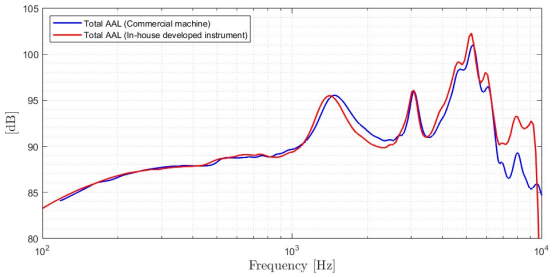

Figure 12: AAL results comparison between the commercial machine and in-house developed instrument.

Both SPL curves follow the profile of measured one. The biggest differences between the two computed SPL curves appears at the points where resonances occur. Taking also in account the same considerations made for the AALs differences, the SPLs differences can also be caused by:

- Phase difference at the reference point considering the real (with its irregularities) or the "ideal" CAD geometry.
- Phase difference due to the sound card latency. Latency is compensated during the post processing step by using `finddelay` MATLAB function and taking a known measured IR as reference. Small phase delays in the measured displacement due to the real loudspeaker behaviour could have been erroneously compensated as if they come from the sound card.

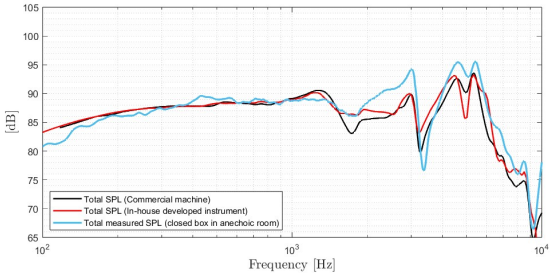

Figure 13: SPL results comparison between the commercial machine and in-house developed instrument. The blue curve is the SPL measured in a closed box (as in figure 9).

A comparison between the components computed with the commercial hardware and with the in-house developed instrument has been analyzed too.

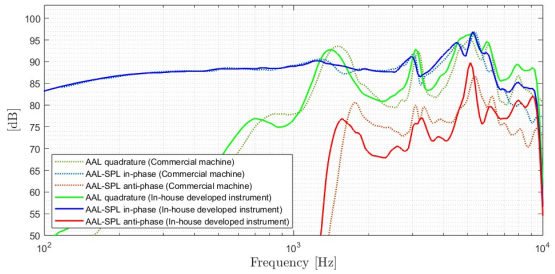

Figure 14: Components results comparison between the commercial hardware and the in-house developed instrument.

Fixing the frequency at 5000 Hz where a dip in the SPL is visible in all result curves, it is possible to compare the components decomposition results. It must be kept in mind that there may be the possibility that the grid radii measured with the commercial instrument may not be placed at the same angle as those measured with in-house developed instrument, thus giving a different result.
In figures 15 and 16 we can observe in the anti-phase component plots (on the top) that point moving in anti-phase are very close to the ones identified by the commercial instrument. Also the in-phase component plots (in the middle) presents several similarities with the one of the commercial instrument. The quadrature component (on the bottom) is the one that most differs from the one obtained with the commercial instrument, although, since in both cases it extends over the entire loudspeaker surface.

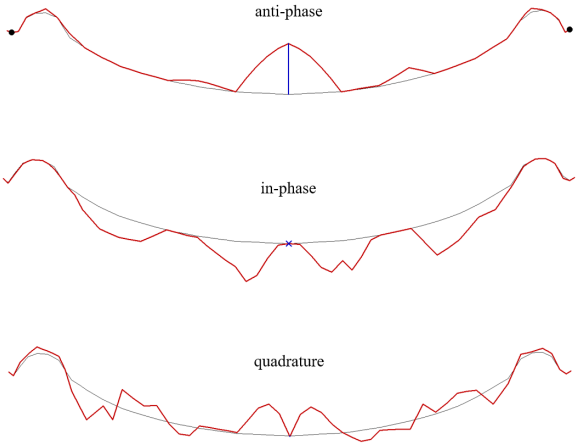

Figure 15: Components graphical decomposition results from the commercial instrument measurement [1].

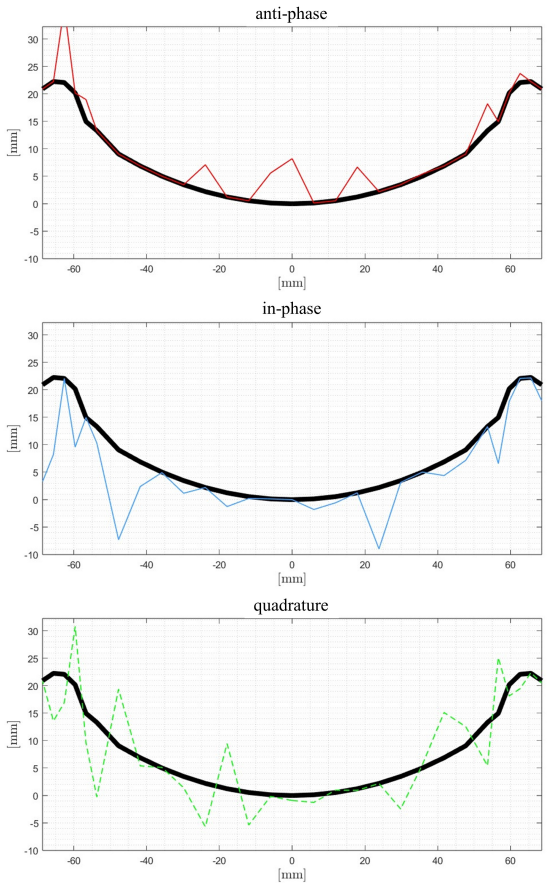

Figure 16: Components graphical decomposition results from in-house developed instrument.

8. Conclusions and future developments

This work goes beyond creating an instrument and highlights the transformative potential of

laser measurements in loudspeaker design. The project demonstrates how essential information for research and product development can be derived from displacement measurements. Previously unavailable information about the modal behaviour of loudspeaker membranes can really help designers to both characterize materials, assess the relative importance of geometry and materials in specific cases, avoiding design flaws, improving products performance while reducing trial-and-error approach. In the future, several improvements can be made to enhance the reliability of the measurement instrument and the accuracy of the results. The currently used sound card should be replaced with an external card with DC voltage reading capabilities to both retrieve the surface profile directly from the laser displacement sensor output and keeping target distance inside the sensor focal range. The measurement and compensation of the sound card and system latency can be done in the measurement phase, improving the accuracy of the results. Multiple measurements can be taken at the same point and averaged to improve the SNR. Additionally, the graphical visualization of components on the cone surface can be improved by adding time dependence and showing the total displacement over time. Finally, a 3D visualization of displacement and components over the loudspeaker surface can be implemented. These future developments aim at enhancing the instrument's capabilities and provide designers with even more valuable insights for loudspeaker design and improvement.

9. Acknowledgements

I would like to extend my sincere appreciation to Eighteen Sound and B&C Speakers for graciously allowing me to conduct my master's thesis at their place. Their support and collaboration have been essential in the successful completion of my research. I am grateful for the valuable insights and assistance provided by their teams, whose dedication and enthusiasm followed me throughout these months.

References

[1] Wolfgang Klippel. Hardware and software module of the klippel scanner analyzer system. *www.klippel.de*, 2022.

[2] Leo Beranek and Tim Mellow. *Acoustics - Sound Fields, Transducers and Vibration.* Academic Press, 2019.

[3] Wolfgang Klippel and Joachim Schlechter. Distributed mechanical parameters describing vibration and sound radiation of loudspeaker drive units. *AES - 125th convention*, 2008.

[4] F. J. M. Frankort. Vibration patterns and radiation behavior of loudspeaker cones. *Audio Engineering Society - Vol.26 No.9*, pages 609–622, 1978.

[5] Pierrick Lotton Antonin Novak and Laurent Simon. Synchronized swept-sine: Theory, application and implementation. *Audio Engineering Society - Vol.63 No.10*, pages 786–798, 2015.

[6] René Christensen. Phase decomposition for loudspeaker analysis. *COMSOL Multiphysics Conference*, 2016.